Determination of the Electron Diffusion Length in Dye-Sensitized Solar Cells by Random Walk Simulation: Compensation Effects and Voltage Dependence

J. P. Gonzalez-Vazquez,[†] Juan A. Anta,*[,†] and Juan Bisquert[‡]

Departamento de Sistemas Físicos, Químicos y Naturales, Universidad Pablo de Olavide, 41013 Sevilla, Spain, and Photovoltaic and Optoelectronic Devices Group, Departament de Física, Universitat Jaume I, 12071 Castelló, Spain

Received: January 29, 2010; Revised Manuscript Received: March 19, 2010

The diffusion length is a crucial parameter controlling the electron collection efficiency in dye-sensitized solar cells (DSCs). In this work, we carry out a direct computation of this parameter for a DSC with a short diffusion length by running a random walk numerical simulation with an exponential distribution of trap states and explicit incorporation of recombination. The diffusion length and the lifetime are estimated from the average distance traveled and the average survival time of the electrons between recombination events. The results demonstrate the well-known compensation effect between diffusion and recombination that keeps the diffusion length approximately constant on a wide range of illumination intensities or applied biases. The assumptions considered in the present model indicate that the two alternative views described in the literature to rationalize this effect (either "dynamic" or "static") are equivalent. As a further development of the model, we introduce a recombination probability that depends exponentially on the Fermi level. This leads to a nonconstant diffusion length, as shown in recent experiments.

1. Introduction

Dye-sensitized solar cells (DSCs)[1,2] are one of the most studied photovoltaic devices nowadays due to their promising features for low-cost solar energy production. A DSC device is based on the combination of three main components: a nanostructured semiconductor oxide (typically TiO_2) that acts as an electron conductor, an organic or metal−organic dye adsorbed onto the oxide surface that absorbs light and injects electrons into the oxide conduction band, and a hole conductor that impregnates the semiconductor nanostructure so that it can regenerate the dye and close the circuit. The good performance of DSCs relies on the favorable dynamic competition[3−5] between these photoinduced processes and other recombination pathways that cause a reduction of the collection efficiency. Among the first, the transport of photogenerated electrons through the semiconductor nanostructure is central for good performance. For a DSC device to work efficiently, photogenerated electrons traveling through the semiconductor nanostructure should be collected to a fraction close to a 100%. The electron diffusion length L_n represents the distance that electrons travel on average before recombining with an electron acceptor. Hence, efficient cells are characterized by L_n values that exceed the semiconductor film thickness.

The electron diffusion length is commonly determined from independent measurements of the electron diffusion coefficient D_n and the electron lifetime τ_n via

$$L_n = (D_n \tau_n)^{1/2} \tag{1}$$

The diffusion length was first introduced by Amaldi and Fermi in 1936 in the context of neutron diffusion in paraffin samples[6] as the distance that "a neutron will diffuse before it gets captured by a proton." In fact, the diffusion length appears in the solution of the 1-D diffusion equation with a single recombination term governed by a certain lifetime τ_n.[7−10] The solution of this equation is exponential, with the diffusion length occurring in the exponent: $\exp(-x/L_n)$. L_n is also the first moment of the probability distribution function, which shows that this parameter corresponds to the average value of the distance traveled by the particles before they disappear by recombination.

Electron transport in nanostructured oxide films impregnated with a highly concentrated electrolyte is believed to occur mainly by diffusion.[11,12] It is generally accepted that this diffusional transport is influenced by the existence of electron localized states or traps in the semiconductor.[13] Trap-limited transport can be described by means of the well-known multiple-trapping (MT) model.[14−16] In this model, transport is assumed to occur via extended states combined with a succession of trapping and detrapping events in localized states.

It has been observed experimentally in common DSCs that the electron diffusion length remains approximately constant on a wide range of illumination intensities or applied biases.[17−19] This behavior arises from the opposite dependences of D_n and τ_n with respect to the applied bias, which makes their product approximately constant. Thus, the diffusion coefficient increases when the illumination is augmented (or a more negative potential is applied). This is easily understood in the context of the MT model because electron injection into the semiconductor film (either from the dye or from the back contact) raises the Fermi level so that the rate of detrapping to the transport level is enhanced. In contrast, the lifetime becomes shorter when the light intensity or the negative applied potential is increased. This is somehow a more complicated effect to rationalize, and two different views can be found in the literature.

On the one hand, it can be assumed that, if the electron transport becomes faster when the Fermi level is raised, then the probability for an electron to find an electron acceptor is larger so that the

* To whom correspondence should be addressed. E-mail: anta@upo.es.
† Universidad Pablo de Olavide.
‡ Universitat Jaume I.

10.1021/jp100874e
Published on Web 04/08/2010

electron lifetime is shortened. We call this interpretation the "dynamic" view, and it can be found in the works of Nelson et al.,[20] Kopidakis et al.,[21] Anta et al.,[22] and Villanueva et al.[23,24] Also, Petrozza and co-workers[25] discussed recombination in connection with this "dynamic" view. On the other hand, a careful analysis of the MT model under the assumption that the rates for trapping and detrapping are much higher than the typical recombination rate, demonstrates that free and trapped electrons maintain a common equilibrium even if the system is perturbed by, for instance, a recombination event. This result is due to Bisquert and Vikhrenko,[15] and we call it the "static" view (in fact, this is usually referred to as the "quasi-static approximation"). Within this formalism, the following dependences can be derived for the diffusion coefficient and the lifetime

$$D_n = \left(\frac{\partial n_c}{\partial n_L}\right) D_0 \tag{2}$$

$$\tau_n = \left(\frac{\partial n_L}{\partial n_c}\right) \tau_0 \tag{3}$$

where n_c and n_L are the concentrations of free and trapped electrons (which depend on the Fermi level) and D_0 and τ_0 are the diffusion coefficient and the lifetime for free electrons. Including eqs 2 and 3 into eq 1, we find that the lifetime is equal to a constant

$$L_n = (D_0 \tau_0)^{1/2} \tag{4}$$

The approximation of Bisquert and Vikhrenko demonstrates that it is not necessary to resort to a dynamic, transport-limited mechanism to explain the observed behavior of the lifetime and the diffusion length because the mechanism involving the variation of these quantities with the Fermi level is associated with the trapping−detrapping of free carriers, and this process is described in eqs 2 and 3 by a single trapping factor, $\partial n_L/\partial n_c$, that accounts for the change of the time constants due to the fraction of the time that the free carriers spend in traps.

A recent study[26] has further clarified the interpretation of eq 3, which has been formulated in the form

$$\tau_n = \left(\frac{\partial n_L}{\partial n_c}\right) \tau_f \tag{5}$$

where τ_f is a free electron lifetime, which is the effective probability of survival of electrons in the conduction band. In general, τ_f depends on the specific recombination mechanism, and it will be a constant if the rate of recombination of free electrons is proportional to their density. However, the recombination mechanism may involve a combination of charge transfer channels, especially due to the contribution of a distribution of surface states.[27,28] In a first approximation, the recombination rate is effectively observed to depend on a power of the free electron density as follows[9,23,29]

$$U_n = k_r n_c^{\beta} \tag{6}$$

where k_r is a recombination kinetic constant. This model implies that the free carrier lifetime shows a dependence on the Fermi level given by[9]

$$\tau_f = \frac{n_0^{1-\beta}}{\beta k_r} \exp\left[\frac{(1-\beta)}{k_B T}(E_F - E_{F,0})\right] \tag{7}$$

with n_0 and $E_{F,0}$ being the equilibrium (dark) values of the electron density and Fermi level, respectively, k_B is the Boltzmann constant, and T is the absolute temperature. According to this model, for $0 < \beta < 1$, the recombination rate increases more slowly with electron density than in the linear case, and thus, the free carrier lifetime increases with the Fermi level. This model has important implications for the variation of the diffusion length with bias illumination or potential in the solar cell.[9] From eqs 1 and 5, we obtain

$$L_n = (D_0 \tau_f)^{1/2} \tag{8}$$

so that it is predicted that the diffusion length should increase with the steady-state Fermi level. As a matter of fact, recent reports on DSCs indicate that the electron diffusion length is not strictly constant, but it increases with applied voltage.[30−33] Specially, the study by Peter and co-workers[10] has carefully determined the variation of L_n at different bias illuminations, and good agreement has been found with the *β-recombination* model of eq 6. These recent reports suggest that equilibration (trapping) factors present in both diffusion coefficient and measured lifetime are essentially the same number, $\partial n_L/\partial n_c$, so that the asymmetry of these two quantities refers to the free electron lifetime, which causes a variation of the diffusion length.

The purpose of this paper is twofold. On the one hand, we pursue to compute the electron lifetime and electron diffusion length for a dye-sensitized solar cell, at potentiostatic conditions (fixed Fermi level) by means of the random walk numerical simulation (RWNS). On the other hand, we intend to cast some light on the origin of the compensating behavior of the electron diffusion length and to establish how the "dynamic" and the "static" views mentioned above are related to each other. We will see that the RWNS method employed here, although based on dynamic postulates (random generation of detrapping and recombination times), reaches a quasi-stationary state that reproduces the theoretical dependences predicted for the diffusion coefficient and the lifetime, hence, explaining the compensation behavior. In addition, the introduction of a recombination probability that depends exponentially on the Fermi level according to eq 7 leads to a nonconstant electron diffusion length, as observed in some experiments.

2. Methodology

The RWNS method[34,35] is a stochastic calculation that makes it possible to obtain dynamic properties (electron mobilities,[16] diffusion coefficients,[21,36,37] photocurrent,[20] and photovoltage transients[38]) in disordered media, starting from basic assumptions about the transport mechanism. In a RW numerical simulation, a number of carriers are allowed to move at random in a three-dimensional network of sites (see Figure 1). According to the selected transport model, each site in the network is given a certain release time that determines the jumping rate or probability for a carrier to jump to another site. If we consider the MT mechanism of charge transport discussed above and no external electric fields, the release time depends only on the energy of the starting site E_i according to the expression[16,34]

$$t_i = -\ln(R) \cdot t_0 \cdot e^{(E_i - E_0)/k_B T} \tag{9}$$

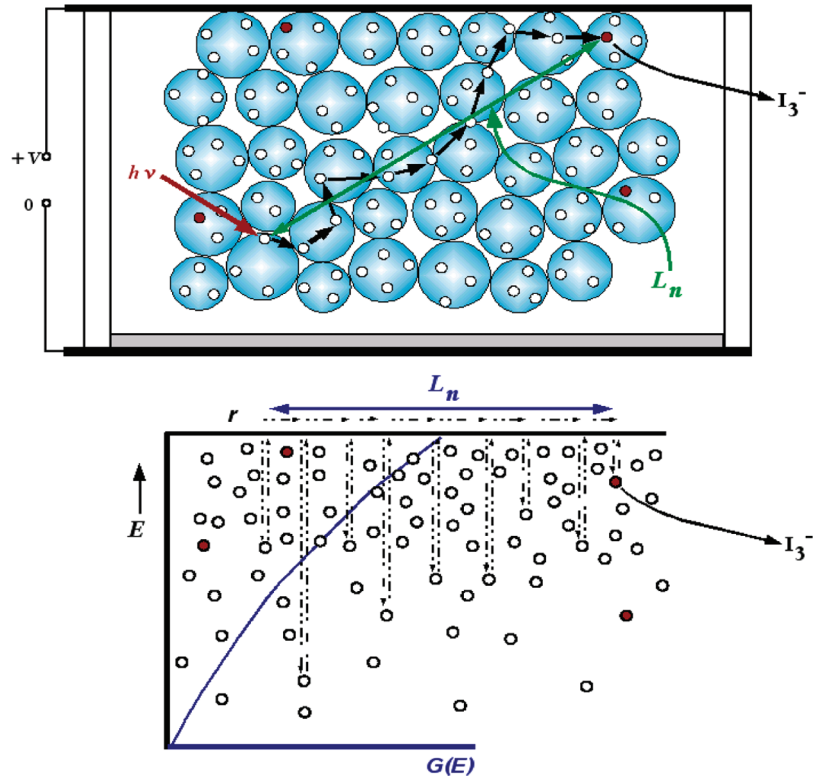

Figure 1. Illustration of the random walk numerical procedure utilized in this work to compute the electron diffusion length L_n. A three-dimensional network of traps is distributed randomly and homogeneously in space. The energies of the sites are taken from an exponential distribution $G(E)$ given by eq 10. A *recombining character* is given to an arbitrary amount of traps (solid circles) so that, when an electron reaches one of these traps, it may undergo recombination (reaction with I_3^-) and be removed from the sample. See text for more details.

where R is a random number uniformly distributed between 0 and 1, E_i is the energy of the site (definite-positive), and E_0 is the energy of the extended state through which transport is assumed to occur, that is, the mobility edge or the conduction band lower bound. In eq 9, t_0 is an adjustable parameter that controls the time scale of the simulation.

In this work, we run the random walk simulation on a three-dimensional network of traps distributed randomly and homogeneously in space. The energies of the sites are taken from the usual exponential distribution[39]

$$G(E) = \frac{N_L}{k_B T_0} \exp[-(E - E_0)/k_B T_0] \qquad (10)$$

where N_L is the total trap density and $k_B T_0$ is the width of the distribution (the mean value of the energy).

Details on the organization of an RW simulation based on times are given elsewhere.[16,35,36,38] In the calculation, electrons are given *release times* according to eq 9 for the energies and positions of the sites they visit. *Waiting times* are defined as the difference between the release time of the carrier and the time already spent by the carrier in a particular site. For each simulation step, the carrier with the shortest waiting time (t_{min}) is allowed to move to a neighboring trap, chosen at random, within the specified cutoff. The waiting times for the rest of the carriers are then reduced by t_{min}; the process is repeated, so the simulation advances by time steps of length t_{min}. This procedure permits sampling efficiently systems characterized by a huge dispersion of site energies, as those derived from eq 10. The computation of the mean square displacement from the electron positions permits obtaining the *jump* diffusion coefficient for each simulation time.[36]

In this work, we have introduced recombination in the basic RW algorithm. Following classic[4,21,40] and recent literature,[10,41] we assume that recombination is mainly determined by trapped electrons. Hence, we give a *recombining character* to an arbitrary amount of traps so that, when an electron reaches one of these traps, it may undergo recombination and be removed from the sample (see Figure 1). In addition, a probability of recombination is implemented for electrons once they reach a recombining trap. Hence, we work with two adjustable parameters, one to compute the relative concentration of recombining traps and the other to compute the probability of recombination once the electron has reached one of these traps. It must be noted that the final result for the electron diffusion length, once the stationary state is reached, depends, as a matter of fact, on the *product* of these two probabilities and not on the individual values. However, by separating the concentration of recombining traps from the probability of recombination with a single trap, we can easily implement different recombination mechanisms, as it will be shown below.

Taking into account this procedure, we compute both the average time and the average distance that an electron is moving until it recombines. To simulate a cell at open-circuit conditions and under illumination (fixed Fermi level), a constant electron density is maintained in the sample. This is achieved by imposing the restriction that, when an electron has just recombined, another one is immediately injected into the system to take its place. For this *fresh* electron, both time and distance are reset so that the average time and distance between recombination events can be computed, stored, and represented versus total simulation time. As the probability of recombination is small (see below), no significant bias is observed in the results when the new electron is generated close to a recombining trap. Finally, these magnitudes are renormalized by the total number

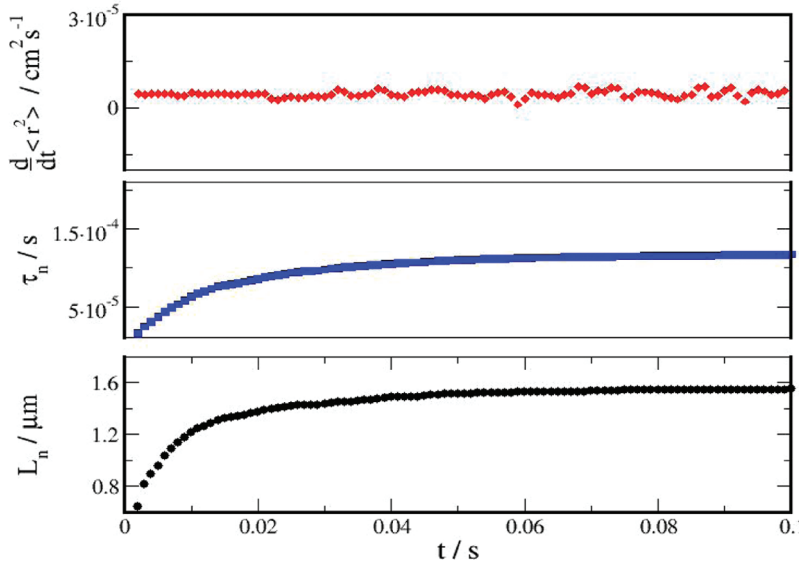

Figure 2. Time evolution of the derivative of the mean square displacement (upper panel), lifetime (middle panel), and electron diffusion length (lower panel) in a typical RWNS calculation carried out in this work. Data shown correspond to a multielectron calculation with 50 electrons in a simulation box of 18 × 18 × 18 nm^3.

of electrons and the total number of recombination events so that the result is effectively an average time and distance for one single electron. We will show below that these averaged quantities effectively correspond to the lifetime and diffusion length of electrons in the sample.

The procedure outlined above permits us to run a multielectron calculation at a fixed density or Fermi level. However, to approach conditions similar to those typical of an operational cell, a huge amount of computer time is required. To save time when computing the electron diffusion length at realistic conditions, most of the simulations presented in this work are carried out with a single electron moving on a truncated exponential distribution. For this modified distribution, all traps below the Fermi level E_F are ignored (see the Supporting Information). In this way, we assume that electrons occupying deep traps are effectively immobilized. We have demonstrated elsewhere[36,10,41] that this procedure reproduces the electron diffusion coefficient of the full calculation with reasonable precision.

It may be argued that the one-electron calculation does not correctly capture the slowing down of the lifetime by the trapping−detrapping process, that is, described in the model by the factor $\partial n_L/\partial n_c$. However, it must be observed that the main limiting factor in the trapping−detrapping dynamics is detrapping from deep traps, and the fastest of such occupied traps are, on average, those at the Fermi level. Therefore, the convenient truncation procedure still keeps the main aspect of the collective dynamics. This conclusion is further supported when the results are compared with those of the time decay of the full population by recombination, as it will be discussed below (see the Supporting Information, Figure S2).

The RWNS procedure devised here allows for simultaneous computation of the electron diffusion coefficient and the electron lifetime and electron diffusion length at the same Fermi level position. We have taken into account parameters reported in the literature[42,30,36] for a DSC with a solid-state hole conductor to carry out our calculations. Hence, we take $t_0 = 10^{-14}$ s, $T_0 = 1100$ K, and $T = 300$ K. The total trap concentration is assumed to be[38,43] $N_L = 10^{27}$ m^{-3}. In addition, one recombining trap is introduced per 64 000 normal traps and a further recombination probability of 0.05 is imposed. Finally a cutoff radius of 2.5 nm is introduced in the computation so that jumps to neighboring traps beyond this distance are not considered. With these parameters, the simulation predicts an electron diffusion length of 1.6 μm, which is consistent with the values reported in the literature[42,30] for this kind of cell.

TABLE 1: Characteristic Times for the One-Electron RWNS Calculations Performed in This Work

E_F/eV	release time from E_F (s)	average lifetime τ_n (s)	total simulation time (s)
0.35	7.7×10^{-9}	$(8.13 \pm 3.50)\cdot 10^{-5}$	0.05
0.45	3.7×10^{-7}	$(1.38 \pm 0.22)\cdot 10^{-3}$	0.5
0.55	1.8×10^{-5}	$(2.22 \pm 0.46)\cdot 10^{-2}$	1
0.65	8.5×10^{-4}	$(3.75 \pm 0.63)\cdot 10^{-1}$	50

3. Results and Discussion

In Figure 2, the time evolution of the derivative of the mean square displacement (related to the jump diffusion coefficient), the lifetime, and the electron diffusion length are reported. It is observed that the simulation reaches rapidly a stationary situation in which the mean square displacement behaves linearly with time (constant time derivative) within the statistical uncertainty of the simulation (normal diffusion). This has been shown to correspond, in multielectron simulations, to the situation in which the electron population reproduces Fermi−Dirac statistics.[36] On the contrary, the lifetime and the diffusion length are found to reach the stationary state at longer times. This is easy to understand if we bear in mind that the characteristic times for detrapping (as derived from eq 9 for electrons sitting at the Fermi level) are much shorter than the characteristic time for recombination (the lifetime). In Table 1, values obtained for these characteristic times are reported. The results demonstrate that the assumptions on which the quasi-static approximation is based (that is, equilibration between free and trapped electrons much faster than recombination) hold in this case. On the other hand, the simulation time is long enough to sample efficiently many recombination events so that the values of the lifetime and the electron diffusion length are estimated correctly.

Results for the diffusion coefficient, the lifetime, and the diffusion length as a function of Fermi level can be found in Figure 3. The RW simulation provides a nice demonstration of

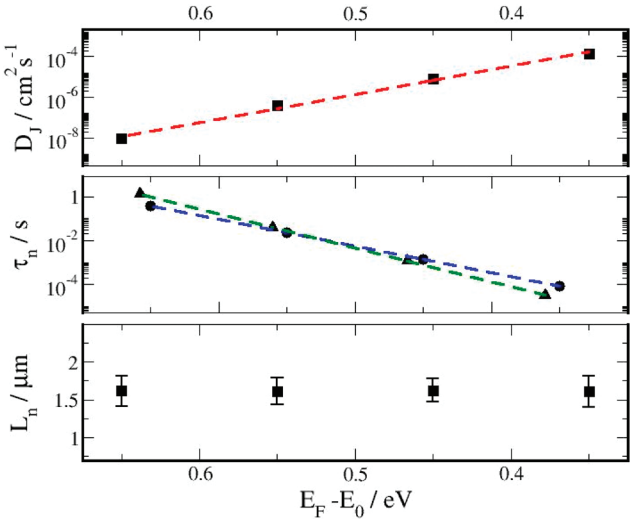

Figure 3. Jump diffusion coefficient (upper panel), electron lifetime (middle panel), and electron diffusion length (lower panel) vs Fermi level. In the middle panel, two methods to compute the electron lifetime are plotted: average of survival times (circles) and time decays (triangles). Note that, due to the logarithmic scale, the error bars fall within the symbol size in the case of the diffusion coefficient and the lifetime.

the compensation effect discussed in the Introduction. The diffusion coefficient scales exponentially with Fermi level, as reported before.[36,44] The slopes obtained from the simulated data were 31.86 and 28.09 eV^{-1} for D_j and τ_n, respectively. These values compare favorably with the predictions of the theoretical formula derived in the context of the MT model[44]

$$D_J = \frac{N_0}{N_L} e^{[(E_F - E_0)(\frac{1}{k_B T} - \frac{1}{k_B T_0})]} D_0 \qquad (11)$$

where N_0 is the density of states in the conduction band.

This equation predicts 28.15 eV^{-1} for $T = 300$ K and $T_0 = 1100$ K. As a consequence of the equal, but opposite, behaviors of D_J and τ_n, the electron diffusion length remains constant within the statistical uncertainty of the simulation, in accordance with the predictions of the diffusion-limited model or the quasi-static approximation.

It is important to establish whether the average lifetime and average diffusion length extracted from the simulations correspond to the real quantities occurring in eqs 1 and 3. As mentioned above, the diffusion length appears in the solution of the 1-D diffusion equation with a first-order recombination term.[7,8] On the other hand, the lifetime is the parameter controlling the exponential time decay of a first-order recombination reaction. To clarify this point, we have computed the distribution of survival times and distances traveled by the electrons before they recombined (see Figure 4). It is found that these distributions do indeed follow an exponential behavior. However, the results obtained for the distribution of distances do not fit to an exponential in the short length region. Ignoring this region in the fitting, we obtain a reasonable agreement between the average value of the diffusion length (1.62 ± 0.15 μm) and that derived from the fitting (1.44 μm). The agreement is more remarkable for the lifetimes: 1.38 ± 0.22 ms (average) versus 1.23 ms (fitting).

The result of this analysis indicates that the average value obtained from the simulation corresponds to the real diffusion length of eq 1. A similar assumption can be established for the

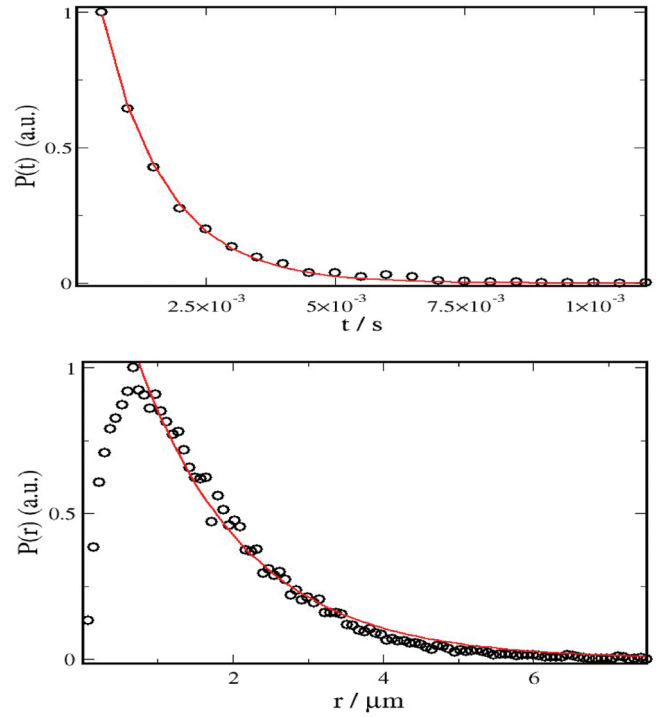

Figure 4. Distribution of survival times (upper panel) and distances traveled by the electrons before recombination (lower panel) as obtained from one-electron RWNS calculations at $E_F = 0.45$ eV. The solid lines stand for fittings to an exponential function. The data are normalized with respect to the first point in the distribution.

TABLE 2: Values of the Chemical Diffusion Coefficient and Lifetime at Different Fermi Levels As Obtained from RW Simulation[a]

E_F/eV	D_n/cm^2 s^{-1}	τ_n/s	L_n/μm (eq *1*)	L_n/μm (RWNS)
0.35	$(5.17 \pm 0.08)\cdot 10^{-4}$	$(8.13 \pm 3.50)\cdot 10^{-5}$	2.05 ± 0.46	1.61 ± 0.21
0.45	$(2.80 \pm 0.42)\cdot 10^{-5}$	$(1.38 \pm 0.22)\cdot 10^{-3}$	1.97 ± 0.30	1.62 ± 0.15
0.55	$(1.37 \pm 0.37)\cdot 10^{-6}$	$(2.22 \pm 0.46)\cdot 10^{-2}$	1.74 ± 0.42	1.61 ± 0.18
0.65	$(3.45 \pm 1.18)\cdot 10^{-8}$	$(3.75 \pm 0.36)\cdot 10^{-1}$	1.14 ± 0.29	1.62 ± 0.20

[a] Values of L_n have been obtained from eq 1 and RW simulation. Note that the diffusion coefficients shown are extracted from the simulated ones according to $D_n = (T_0/T)D_J$.

lifetime. However, it must be borne in mind that this is normally introduced as a collective magnitude, defined from kinetic equations based on total densities. We should then distinguish between the individual magnitudes (computed by the simulation) and collective parameters in analogy with the distinction between "jump" and "chemical" diffusion coefficients introduced by Bisquert.[45] Note, in this regard, that a simple relationship is found for the chemical diffusion coefficient if the trap distribution is exponential, $D_n = (T_0/T)D_J$. This relation states that the Fermi level dependence of both diffusion coefficients is the same, at least for an exponential distribution. We might think that the same relation holds for the lifetimes because an exponential behavior with respect to the Fermi level is obtained.

However, as it will be shown below by multielectron calculations, this lifetime is observed to correspond to the collective lifetime τ_n. Hence, we can compare directly the electron diffusion length obtained from the simulation average to that derived from eq 1. Results can be found in Table 2.

We observe that the diffusion length obtained "indirectly" does not preserve the constancy with respect to the Fermi level. This is a consequence of the fact that, due to the statistical uncertainty of the simulation, the slopes obtained for D_j and τ_n

are not exactly equal. In any case, our results show that the individual quantities maintain the same behavior that their "chemical" counterparts, hence, the compensation behavior predicted by the theories.

The determination of the lifetime, above, has been obtained from direct computation of the survival time of the electron population. However, experimentally, the lifetime is usually obtained by monitoring the decay of the Fermi level. To provide further support to the method employed here to compute the electron lifetime, we have carried out multielectron random walk simulations aimed to resemble a typical open-circuit voltage decay experiment.[46,47] Hence, we have run simulations with an initial number of electrons that corresponds approximately to the Fermi levels studied in Table 2 and with no energy cutoff in the trap energy distribution. The calculation is performed with the same recombination features as in the one-electron simulations (same concentration of recombining traps and same probability of recombination). However, in this case, no new electrons are introduced after recombination so that the concentration of electrons in the sample decreases with time (see the Supporting Information). This is a random walk method analogous to that used by Petrozza et al.[25] The analysis of this decay at short times shows that it is exponential, and the numerical fitting yields an approximate value of the lifetime at the corresponding value of the Fermi level. Results are shown in Figure 3 (middle panel, triangles) and in the Supporting Information. It is observed that the lifetimes reproduce quite accurately the values obtained from the "average" method. The new diffusion lengths shown in Table S1 (Supporting Information) also remain approximately constant, within the statistical error, upon Fermi level variation.

At this point, it is important to discuss the two "views" presented at the beginning of this paper. We must take into account that the RWNS procedure is a dynamic method in which electrons move on a random network of traps within a certain time span. If the Fermi level is raised, the electrons move faster on average, and therefore, they are more likely to encounter a recombining trap. This explains why the lifetime becomes shortened when the Fermi level is raised and supports apparently the "dynamic" view of the recombination process. However, it must be taken into account that the simulation reaches, at a certain time, a stationary situation in which the diffusion coefficient (earlier) and the lifetime (later) remain constant for the same Fermi level. In multielectron calculations, this situation is found to correspond to a situation in which the electron population relaxes to the equilibrium Fermi distribution.[36] Hence, the results provided by the simulation arise from the fact that the system is at internal equilibrium with a trapping−detrapping rate that is much faster than the characteristic recombination time. Therefore, the "static" view in which diffusion coefficient and lifetime arise from a quasi-equilibrium with a well-defined Fermi level is in accordance with the results analyzed here.

On the basis of the preceding results, we can further discuss the interpretation of transport and recombination in a DSC according to the two approaches that have been used in the literature. The transport-limited recombination is a statement that recombination becomes faster (shorter lifetime) as transport becomes faster. Inherent to multiple-trapping mechanisms is a displacement of electrons in the conduction band. Given a distribution of recombining traps, the only factor causing an acceleration of recombination at higher Fermi levels is the progressive filling of deep traps, but this is precisely the same process causing the acceleration of the transport rate. Indeed,

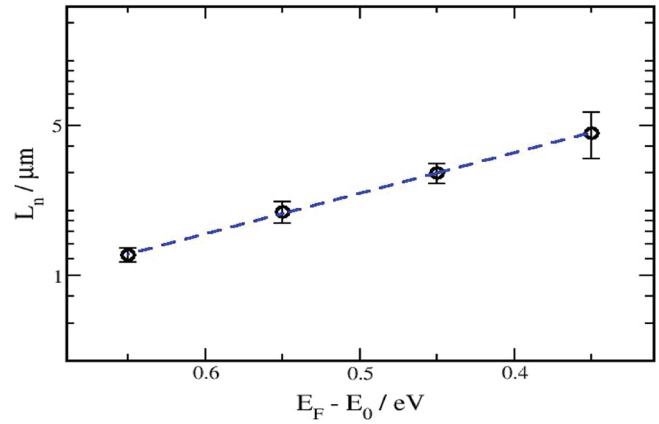

Figure 5. Electron diffusion length extracted from the RWNS calculation with a probability of recombination that depends on the Fermi level according to eq 12.

transport-limited recombination and the quasi-static model describe a unique model, although the latter approach has the advantage that the dependence is quantified via eqs 2 and 3. In none of the approaches it is suggested that recombination depends on the velocity of free carriers (as in Langevin recombination). This mechanism should propose that the rate constant for recombination depends on D_0, and this has not been contemplated so far in the literature because the role of traps indeed provides the main influence on the measured quantities.

As discussed in the Introduction, recombination shows additional features (i.e., a power-law dependence on free electron density) to those derived from the simple multiple-trapping description.[9,10,23,25] This means that the compensation effect that we have just demonstrated will be only partly satisfied and the electron diffusion length is not a constant. With the aim of reproducing this experimental feature, we have modified our model by introducing an additional feature: a recombination probability that depends on Fermi level position. Therefore, we assume, according to eq 7, that the Fermi-level-dependent probability of recombination for an electron reaching a recombining trap is given by

$$P_{\mathrm{rec}}(E_{\mathrm{F}}) = A\mathrm{e}^{(1-\beta)(E_{\mathrm{F}}-E_0)/k_{\mathrm{B}}T} \qquad (12)$$

and β is adjusted to $\beta = 0.77$.[26] On the other hand, the prefactor A is adjusted to give a diffusion length of approximately[30] 3 μm at $E_{\mathrm{F}} - E_0 = 0.45$ eV. According to this expression, electrons are less likely to recombine when the Fermi level approaches the conduction band. As a consequence, the diffusion length increases accordingly, as shown in Figure 5. The slope obtained from the log $L_n - E_{\mathrm{F}}$ plot is 4.36 eV^{-1}, which is very close to the value predicted in ref 26: $\beta/(2k_{\mathrm{B}}T)$ for $T = 300$ K and $\beta = 0.77$.

The one-electron calculations utilized here to obtain realistic values of the electron diffusion length and its voltage dependence correspond, in reality, to an effective procedure in which the Fermi level is fixed and taken as an input to the calculation. A more fundamental way of computing the lifetime and the diffusion length would require running multielectron calculations on the full trap distribution with energy-dependent recombination probabilities. As mentioned above, this computation is quite costly from the numerical point of view (around 40 h of CPU time for a single run, with around 50−100 runs required to get good statistics).. However, in order to test the feasibility of the multielectron simulation with explicit consideration of recom-

bination, a preliminary calculation has been performed for a total electron density that corresponds approximately to $E_F - E_0 = 0.45$ eV. In this calculation, the probability of recombination is made to depend exponentially on the trap energy, as in eq 12. We have found that it is possible to reproduce the same electron diffusion length (see the Supporting Information, Figure S3) as in the one-electron calculation by adjusting the A and β parameters in this expression. This preliminary result encourages us to perform an extensive study with multielectron calculations and explicit recombination mechanisms on the behavior of the electron diffusion length for different electrode materials, electrolyte compositions, etc.

4. Conclusion

One-electron random walk simulations within the multiple-trapping approach have been carried out. Direct computation of the diffusion length has been implemented, and values of the order of micrometers have been obtained for realistic parameters extracted from recent literature. We find that the diffusion length maintains a constant value upon Fermi level variation. Electron lifetimes at different densities have also been computed, and we have obtained an exponential dependence with respect to the Fermi level, producing linear log plots with slopes quite similar, although with opposite sign, also in agreement with previous experimental and theoretical studies. The numerical method and the results obtained in this work indicate that both the "dynamic" and the "static" views to explain recombination in DSCs are indeed equivalent. By introducing, as an additional feature, a probability of recombination that depends exponentially on the Fermi level, a nonconstant electron diffusion length can be reproduced, as observed in recent experiments. Extensive multielectron RWNS calculations that take into account this effect from a more fundamental point of view and with explicit consideration of different molecular recombination mechanisms are now carried out in our group and will be reported in a subsequent publication.

Acknowledgment. We thank the Ministerio de Ciencia e Innovación of Spain for funding under project HOPE CSD2007-00007 (Consolider-Ingenio 2010) and CTQ2009-10477, Junta de Andalucía under projects P06-FQM-01869, P07-FQM-02595, and P07-FQM-02600, and Generalitat Valenciana under project PROMETEO/2009/058.

Supporting Information Available: Three figures and a table showing additional information. This material is available free of charge via the Internet at http://pubs.acs.org.

Note Added after ASAP Publication. This article was published ASAP on April 8, 2010. A value for beta in the text immediately following eq 12 was incorrect. The correct version was published on April 15, 2010.

References and Notes

(1) O'Regan, B.; Gratzel, M. *Nature* **1991**, *353*, 737–740.
(2) Gratzel, M. *Nature* **2001**, *414*, 338–344.
(3) Grätzel, M. *J. Photochem. Photobiol., A* **2004**, *164*, 3–14.
(4) Peter, L. M. *J. Phys. Chem. C* **2007**, *111*, 6601–6612.
(5) Hamann, T. W.; Jensen, R. A.; Martinson, A. B. F.; Ryswyk, H. V.; Hupp, J. T. *Energy Environ. Sci.* **2008**, *1*, 66–78.
(6) Amaldi, E.; Fermi, E. *Phys. Rev.* **1936**, *50*, 899.
(7) Harrick, N. J. *J. Appl. Phys.* **1956**, *27*, 1439–1442.
(8) Bisquert, J. *J. Phys. Chem. B* **2002**, *106*, 325–333.
(9) Bisquert, J.; Mora-Seró, I. *J. Phys. Chem. Lett.* **2010**, *1*, 450–456.
(10) Villanueva-Cab, J.; Wang, H.; Oskam, G.; Peter, L. M. *J. Phys. Chem. Lett.* **2010**, *1*, 748–751.
(11) Sodergren, S.; Hagfeldt, A.; Olsson, J.; Lindquist, S. E. *J. Phys. Chem.* **1994**, *98*, 5552–5556.
(12) van de Lagemaat, J.; Benkstein, K. D.; Frank, A. J. *J. Phys. Chem. B* **2001**, *105*, 12433–12436.
(13) deJongh, P. E.; Vanmaekelbergh, D. *Phys. Rev. Lett.* **1996**, *77*, 3427–3430.
(14) Tiedje, T.; Rose, A. *Solid State Commun.* **1981**, *37*, 49–52.
(15) Bisquert, J.; Vikhrenko, V. S. *J. Phys. Chem. B* **2004**, *108*, 2313–2322.
(16) Anta, J. A.; Nelson, J.; Quirke, N. *Phys. Rev. B* **2002**, *65*, 125324.
(17) Fisher, A. C.; Peter, L. M.; Ponomarev, E. A.; Walker, A. B.; Wijayantha, K. G. U. *J. Phys. Chem. B* **2000**, *104*, 949–958.
(18) Peter, L. M.; Wijayantha, K. G. U. *Electrochem. Commun.* **1999**, *1*, 576–580.
(19) Nakade, S.; Saito, Y.; Kubo, W.; Kitamura, T.; Wada, Y.; Yanagida, S. *J. Phys. Chem. B* **2003**, *107*, 8607–8611.
(20) Nelson, J.; Haque, S. A.; Klug, D. R.; Durrant, J. R. *Phys. Rev. B* **2001**, *63*, 205321.
(21) Kopidakis, N.; Benkstein, K. D.; van de Lagemaat, J.; Frank, A. J. *J. Phys. Chem. B* **2003**, *107*, 11307–11315.
(22) Anta, J. A.; Casanueva, F.; Oskam, G. *J. Phys. Chem. B* **2006**, *110*, 5372–5378.
(23) Villanueva-Cab, J.; Oskam, G.; Anta, J. *Sol. Energy Mater. Sol. Cells* **2010**, *94*, 45–50.
(24) Villanueva, J.; Anta, J. A.; Guilleń, E.; Oskam, G. *J. Phys. Chem. C* **2009**, *113*, 19722–19731.
(25) Petrozza, A.; Groves, C.; Snaith, H. J. *J. Am. Chem. Soc.* **2008**, *130*, 12912–12920.
(26) Bisquert, J.; Fabregat-Santiago, F.; Mora-Seró, I.; Garcia-Belmonte, G.; Gimeńez, S. *J. Phys. Chem. C* **2009**, *113*, 17278–17290.
(27) Bisquert, J.; Zaban, A.; Salvador, P. *J. Phys. Chem. B* **2002**, *106*, 8774–8782.
(28) Salvador, P.; Hidalgo, M. G.; Zaban, A.; Bisquert, J. *J. Phys. Chem. B* **2005**, *109*, 15915–15926.
(29) Wang, Q.; Ito, S.; Gratzel, M.; Fabregat-Santiago, F.; Mora-Sero, I.; Bisquert, J.; Bessho, T.; Imai, H. *J. Phys. Chem. B* **2006**, *110*, 25210–25221.
(30) Fabregat-Santiago, F.; Bisquert, J.; Cevey, L.; Chen, P.; Wang, M.; Zakeeruddin, S. M.; Grätzel, M. *J. Am. Chem. Soc.* **2009**, *131*, 558–562.
(31) Wang, H.; Peter, L. M. *J. Phys. Chem. C* **2009**, *113*, 18125–18133.
(32) Barnes, P. R. F.; Anderson, A. Y.; Koops, S. E.; Durrant, J. R.; O'Regan, B. C. *J. Phys. Chem. C* **2009**, *113*, 1126–1136.
(33) Barnes, P. R. F.; Liu, L.; Li, X.; Anderson, A. Y.; Kisserwan, H.; Ghaddar, T. H.; Durrant, J. R.; O'Regan, B. C. *Nano Lett.* **2009**, *9*, 3532–3538.
(34) Nelson, J. *Phys. Rev. B* **1999**, *59*, 15374–15380.
(35) Anta, J. A. *Energy Environ. Sci.* **2009**, *2*, 387–392.
(36) Anta, J. A.; Mora-Sero, I.; Dittrich, T.; Bisquert, J. *Phys. Chem. Chem. Phys.* **2008**, *10*, 4478–4485.
(37) Anta, J. A.; Morales-Florez, V. *J. Phys. Chem. C* **2008**, *112*, 10287–10293.
(38) Anta, J. A.; Mora-Sero, I.; Dittrich, T.; Bisquert, J. *J. Phys. Chem. C* **2007**, *111*, 13997–14000.
(39) Bisquert, J.; Fabregat-Santiago, F.; Mora-Sero, I.; Garcia-Belmonte, G.; Barea, E. M.; Palomares, E. *Inorg. Chim. Acta* **2008**, *361*, 684–698.
(40) Nelson, J.; Chandler, R. E. *Coord. Chem. Rev.* **2004**, *248*, 1181–1194.
(41) Jennings, J. R.; Wang, Q. *J. Phys. Chem. C* **2010**, *114*, 1715–1724.
(42) Wang, M.; Chen, P.; Humphry-Baker, R.; Zakeeruddin, S.; Gratzel, M. *ChemPhysChem* **2009**, *10*, 290–299.
(43) Fabregat-Santiago, F.; Mora-Sero, I.; Garcia-Belmonte, G.; Bisquert, J. *J. Phys. Chem. B* **2003**, *107*, 758–768.
(44) Bisquert, J. *Phys. Chem. Chem. Phys.* **2008**, *10*, 1–20.
(45) Bisquert, J. *J. Phys. Chem. B* **2004**, *108*, 2323–2332.
(46) Zaban, A.; Greenshtein, M.; Bisquert, J. *ChemPhysChem* **2003**, *4*, 859–864.
(47) Bisquert, J.; Zaban, A.; Greenshtein, M.; Mora-Sero, I. *J. Am. Chem. Soc.* **2004**, *126*, 13550–13559.

JP100874E